Frequency-dependent damping constant and the linewidth of resonant Brillouin scattering of exciton-polaritons in CdS

T. Shigenari,* X. Z. Lu, and H. Z. Cummins
Department of Physics, The City College of the City University of New York, New York, New York 10031
(Received 13 January 1984)

The linewidths of Brillouin components involving lower-branch A-exciton polaritons in the resonant-Brillouin-scattering (RBS) spectrum of CdS have been carefully measured and analyzed. It was found that the exciton damping constant γ must be frequency dependent to explain the observed increase of the linewidth in the resonance region. In particular we suggest that mixing of the $\Gamma_5(A)$ polariton and $\Gamma_6(A)$ exciton states induced by the k-linear interaction is the most probable explanation for the observed sharp increase of the linewidth slightly above the exciton resonance frequency. Interpretation of our linewidth data based on this mechanism led to a coefficient for the k-linear term for the A exciton of $\phi_A=(1.9\pm0.2)\times10^{-11}$ eV cm. The frequency-dependent damping constant $\gamma(\omega)$ must also be used to analyze the intensity of RBS which is related to the additional-boundary-condition (ABC) problem. Preliminary results of intensity fitting using a generalized form of the ABC are presented.

I. INTRODUCTION

Since the pioneering paper by Brenig, Zeyher, and Birman (BZB),[1] many resonant-Brillouin-scattering (RBS) experiments have been performed on semiconductors such as GaAs, CdS, and CdSe.[2] It was shown that the kinematics of RBS (i.e., the dependence of the Brillouin shift on laser frequency) is very well fitted by the BZB theory, which allowed us to determine parameters such as the effective exciton mass m^*, the exciton-photon coupling constant $4\pi\alpha_0$, the transverse resonance frequency ω_T, and the background dielectric constant ϵ_b of CdS from our previous RBS experiments.[3] However, other interesting and important dynamical quantities such as the Brillouin linewidth and intensity have not yet been clarified.

Brillouin-linewidth measurements were reported by Weisbuch and Ulbrich[4] for GaAs, by Hermann and Yu[4] for CdSe, and by Wicksted *et al.*[3,5] for CdS. Significant disagreement with the predictions of the BZB theory with a frequency-independent damping term was noted. On the other hand, the bottleneck effect[6] of exciton-polaritons observed in luminescence spectra indicates that the lifetime of polaritons changes considerably in the region of the resonance frequency.[7,8] Furthermore, it was proposed by Yu that the damping constant should be proportional to k^2 where k is the polariton wave vector.[2] To date, however, no systematic investigations of RBS linewidths have been reported, primarily because of the difficulty of the experiments.

RBS intensity has been studied fairly extensively because it is sensitive to the additional boundary condition (ABC) which determines the relative intensity of the two degenerate polaritons that exist in spatially dispersive media.[9] The intensity, however, depends not only on the ABC, but on other factors such as the dead-layer thickness as well.[10] Recent numerical calculations by Matsushita *et al.* have shown that, even in the absence of a dead layer, the RBS intensity depends strongly on the damping constant γ.[11] Therefore, it is crucial to know the frequency dependence of γ before one attempts to use RBS-intensity data to resolve the ABC problem.

In this paper, we report an extension of our previous experiments to the measurement and analysis of the linewidth of RBS components from the lower-branch (branch 2) A-exciton polaritons in CdS. We discuss different forms for $\gamma(\omega)$ and propose a new line-broadening mechanism—the decay of Γ_5 polaritons into Γ_6 dipole-forbidden excitons via the k-linear interaction.[12] The experiments are reviewed in Sec. II. Results of the linewidth analysis are presented in Sec. III. A preliminary result on the fitting of our RBS-intensity data using the $\gamma(\omega)$ obtained from the linewidth data and a generalized ABC recently proposed by Nakayama[13] is also given in Sec. III. In Sec. IV we discuss the problem of polariton lifetime as well as other possible explanations for the observed frequency dependence of the Brillouin linewidth. Throughout this paper we will use $\tilde{\omega}=\omega/2\pi c$ to represent frequencies expressed in cm^{-1}, with a similar definition for the damping constant $\tilde{\gamma}$.

II. EXPERIMENT

Most of the experimental configuration for the present experiments was identical to that described in Ref. 3. A Kr-laser-pumped single-mode cw dye laser (Coumarin 102 dye) provided the incident light. Backscattered light was collected in a solid angle (outside the crystal) of $10^{-2}\pi$ sr. The angle of incidence was approximately 6°. In the resonance region the refractive index n was about 7.5, and thus the range of internal scattering angles was $\approx179.2°\pm0.8°$. Therefore, line broadening due to finite-collection-angle effects was less than 5×10^{-5} of the Brillouin shift and can be ignored.

Scattered light was first focused onto a 200-μm pinhole to define the scattering volume. Light transmitted through the pinhole was collimated and analyzed by a triple-pass Fabry-Perot interferometer followed by a double-grating spectrometer. The spectrometer functions as a tunable narrow-bandpass filter selecting the desired frequency range out of the complicated spectrum inherent in RBS. This arrangement eliminates overlapping of anti-Stokes components as well as luminescence and Raman scattering into the Stokes 2-2′ Brillouin spectrum which could cause line-shape distortion. The free spectral range (FSR) used in most of the present work was from 8 to 14 cm^{-1}, giving an instrumental linewidth of about 0.2 cm^{-1}. Below the resonance region where the lines are very narrow, a smaller FSR (1 to 4 cm^{-1}) was used to measure linewidths.

The sample was the same type of vapor-grown single-crystal platelet used in Ref. 3. Other crystals which are thought to be of poorer quality gave less reproducible data and linewidths which tended to increase considerably at higher frequencies ($\omega > \omega_L$, where ω_L is the longitudinal exciton frequency at $k=0$). However, the general behavior of the linewidth described in the following section was similar for all the samples studied.

The major differences in the apparatus from the description in Ref. 3 were the decrease of the laser power from 20 to 8 mW and the installation of a more rigid cryostat support which improved mechanical stability and reduced vibrational movement of the sample. The single-mode laser output, polarized perpendicular to the c axis, was focused onto the crystal surface by a lens with a focal length of 160 mm. Above the resonance frequency a slight local heating effect was observed as an increase of Brillouin shift with increasing laser power. We chose 8 mW as a compromise between reducing local heating and maintaining suitable signal intensity. With 8 mW laser illumination we confirmed that local heating does not give rise to inhomogeneous broadening of the Brillouin components by reducing the pinhole from 200 to 10 μm, which reduced the area of the crystal from which scattered light was collected; no change in linewidth was observed.

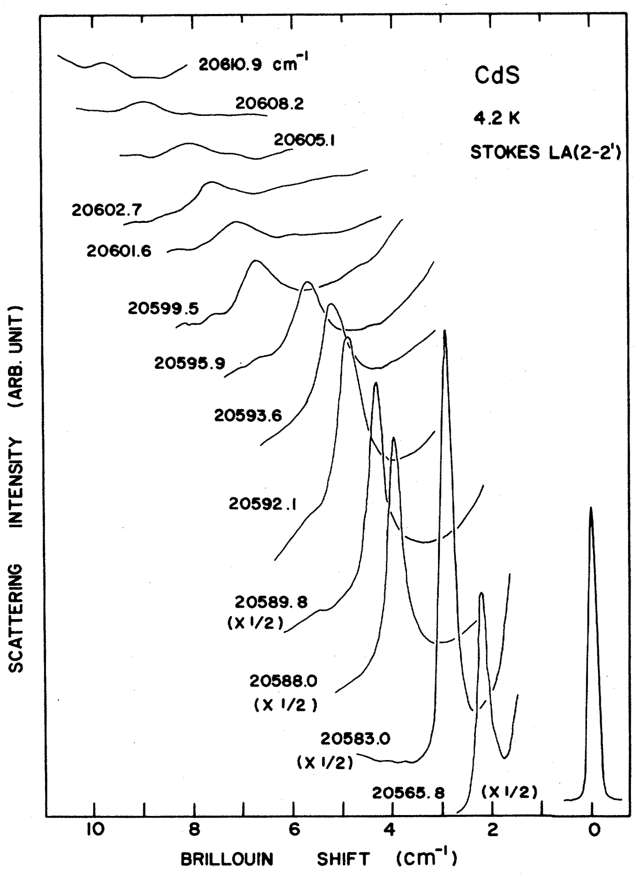

FIG. 1. Brillouin scattering spectra of CdS showing Stokes 2-2′ longitudinal-acoustic (LA) components for various incident laser frequencies. The free spectral range is 13.285 cm^{-1}. The elastic scattering peak indicates the instrumental linewidth. Note that the true intensity for the lowest four spectra is twice as large as shown in the figure.

III. RESULTS

A. Linewidth of Stokes LA 2-2′ Brillouin component

We have concentrated on LA 2-2′ scattering rather than TA 2-2′ scattering, as studied in Ref. 3, because the LA 2-2′ component has the largest Brillouin shift and can be studied over the largest range of laser frequencies. Moreover, the LA linewidth is approximately twice as large as the TA linewidth and therefore allows more accurate linewidth determination. The full width at half max-

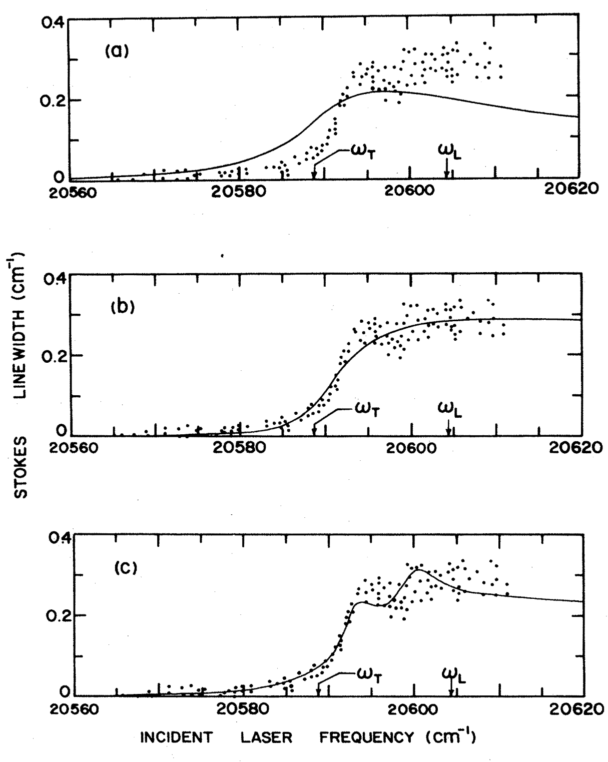

FIG. 2. Stokes LA 2-2′ Brillouin linewidth vs incident laser frequency. The dots are the corrected experimental data. The solid line in (a) is the best fit to model I with $\tilde{\gamma}_0=0.625$ cm^{-1}. The solid line in (b) is the best fit to model II using Eq. (7) with $\tilde{\gamma}_0=0.117$ cm^{-1} and $\tilde{\gamma}_1=0.345$ cm^{-1}. The solid line in (c) is the best fit to model III using Eq. (12) with $\tilde{\gamma}_0=0.241$ cm^{-1}, $\tilde{\gamma}_1=0.091$ cm^{-1}, and $\tilde{\gamma}_2=2.691$ cm^{-1}.

imum (FWHM) of each Brillouin component was obtained by subtracting the average Rayleigh linewidth from the observed Brillouin linewidth, assuming that both lines are Lorentzian. Deconvolution of the line shape was not performed.

Figure 1 shows the change in the LA 2-2′ Brillouin component as the incident laser frequency was varied from below $\tilde{\omega}_T=20\,588.8$ cm^{-1} to above $\tilde{\omega}_L=20\,604.4$ cm^{-1}. The observed Brillouin shifts agree well with our previous data,[3] and in the following analysis we used the parameters $m^*=0.83m_0$, $4\pi\alpha_0=0.0142$, and $\epsilon_b=9.38$, as determined in Ref. 3.

The experimentally observed linewidths (after subtraction of the instrumental linewidth) are shown by the dots in the Figs. 2(a)—2(c), while the solid lines are calculated linewidths based on three different models for $\gamma(\omega)$, to be discussed below. For laser frequencies well below ω_T, the linewidth is small and close to the limit of resolution when the FSR of the Fabry-Perot interferometer is large (8 to 14 cm^{-1}). However, these linewidths were also measured with high resolution (a FSR of about 1.2 to 4 cm^{-1}) and found to be independent of the FSR used in the measurement, in contrast to the results of Flynn and Geschwind.[14]

The observed linewidth increases from 0.03 to about 0.3 cm^{-1} within a narrow range of laser frequencies between 20 585 and 20 595 cm^{-1} and remains approximately constant for higher frequencies. Although the data at high laser frequencies exhibits considerable fluctuation, a slight decrease in linewidth around 20 598 cm^{-1} was observed repeatedly in several series of experiments and is believed to be a real effect.

The differential cross section for Stokes RBS from the ith to the jth polariton branch is given by[11]

$$\left[\frac{d^2\sigma}{d\Omega\,d\omega}\right]_{i\to j}=[1+n_{\rm ph}(\omega_I-\omega_S)]\left[\frac{s_a}{(2\pi)^3(\hbar c)^2C_s}\right]T_i(\omega_I)T_j(\omega_S)[\omega_S^2\,|\,A_{ij}(k_{Ii},k_{Sj})\,|^2]$$
$$\times\left[\frac{|\,\Gamma_0(q=k'_{Ii}-k'_{Sj})\,|^2}{v_{Ei}(\omega_I)\,|\,v_{Gj}(\omega_S)\,|}\right]\left[1\Big/\left\{\left[k'_{Ii}+k'_{Sj}-\left[\frac{\omega_I-\omega_S}{C_s}\right]\right]^2+(k''_{Ii}+k''_{Sj})^2\right\}\right],\tag{1}$$

where $T(\omega)$ is the ABC-dependent transmissivity of photons at the crystal surface, v_E and v_G are the energy and group velocities of polaritons, C_s is the sound velocity, and S_a is the illuminated area of the crystal surface. $k_I=k'_I+ik''_I$ and $k_S=k'_S+ik''_S$ are the complex wave vectors of the incident and scattered polaritons, respectively, A_{ij} is the exciton-strength function, and $\Gamma_0(q)$ is the exciton-phonon—interaction kernel. In the present case (i.e., backward scattering by LA phonons via the deformation-potential interaction), $\Gamma_0(q)$ is proportional to the square root of the phonon wave vector q. For the derivation and notation of Eq. (1), see Ref. 11.

Since the last factor of Eq. (1) is the only one which depends strongly on frequency, the scattered spectrum is expected to have a Lorentzian line shape with a maximum at

$$\omega_S=\omega_I-C_s(k'_{Ii}+k'_{Sj}),\tag{2}$$

and a FWHM of

$$\Delta=2C_s(k''_{Ii}+k''_{Sj}).\tag{3}$$

As originally pointed out by Sandercock, this linewidth is determined by the uncertainty of the phonon wave vector q, and $(k''_I+k''_S)^{-1}$ represents the effective scattering length in which RBS takes place.[15] Damping of the acoustic phonons, which would also contribute to the linewidth, can be neglected at liquid-helium temperature.

By introducing a phenomenological damping constant γ, the complex polariton wave vector $\vec{k}$ can be shown to be related to the real frequency ω by the following equation:[10]

$$\frac{c^2k^2}{\omega^2}=\epsilon_b+\left[\frac{4\pi\alpha_0}{\omega_T^2-\omega^2+Bk^2-i\omega\gamma}\right],\tag{4}$$

where $B=\hbar\omega_T/m^*$. Detailed numerical calculations show that the dispersion curve $k'(\omega)$ (and therefore the Brillouin shift $\omega_S-\omega_I$) is very insensitive to γ as long as it is smaller than a critical value, which is $\tilde{\gamma}\approx 11$ cm^{-1} in the case of the A exciton in CdS.[11] The exciton-strength function A_{ij} and the energy and group velocities in Eq. (1) are also insensitive to γ. On the other hand, $k''(\omega)$ and $T(\omega)$ depend strongly on γ in the resonance region.[16] Therefore, the linewidth given by Eq. (3) and the integrated intensity given by

$$\left[\frac{d\sigma}{d\omega}\right]_{i\to j}=\left[\frac{\pi S_a}{(2\pi)^3(\hbar c)^2}\right]T_i(\omega_I)T_j(\omega_S)$$
$$\times\frac{\omega_S^2\,|\,A_{ij}\,|^2\,|\,\Gamma_0(q)\,|^2}{v_{Ei}(\omega_I)\,|\,v_{Gj}(\omega_S)\,|}\left[\frac{1}{k''_{Ii}+k''_{Sj}}\right]$$
$$\times[1+n_{\rm ph}(\omega_I-\omega_S)]\tag{5}$$

are both sensitive functions of the damping constant γ.

We have considered three contributions to γ corresponding to different decay mechanisms of the polariton in our attempt to determine $\gamma(\omega)$ from the measured linewidths. These are (i) a frequency-independent damping constant γ_0, (ii) a damping constant proportional to the polariton density of states corresponding to decay via elastic scattering, and (iii) damping due to the decay of $\Gamma_{5T}(A)$ polaritons to $\Gamma_6(A)$ excitons via a wave-vector-induced mixing of states which is significant only in the resonance region.

Model I, consisting of the frequency-independent γ_0 alone, is the simplest approximation. γ_0 can represent both radiative recombination and the decay of polaritons to other exciton branches or localized states via interaction with defects, internal stress, etc., because such interactions can scatter a polariton regardless of its wave vector or energy. The solid curve in Fig. 2(a) is the calculated best fit to model I, with

$$\tilde{\gamma}_0=0.625\ \mathrm{cm}^{-1}\ . \tag{6}$$

Obviously, the steep increase of the linewidth just above ω_T cannot be explained by γ_0 alone.

Decay of polaritons via intrabranch elastic scattering can be taken into account by including term (ii) since the transition probability for elastic scattering is roughly proportional to the density of states at energy ω if the detailed ω and/or $\vec{q}$ dependence of the interaction is neglected. Assuming that the energy difference between the initial and final states of the scattering event is sufficiently small (i.e., elastic scattering or scattering by acoustic phonons is dominant), and also neglecting the anisotropy of the CdS wurtzite structure, the density of states is proportional to $k'(\omega)^2/|v_G(\omega)|$. In model II we have included both terms (i) and (ii) with a total $\gamma(\omega)$ given by

$$\gamma(\omega)=\gamma_0+\gamma_1\left[\frac{k'(\omega)}{k_0}\right]^2\left[\frac{v_{G_0}}{|v_G(\omega)|}\right], \tag{7}$$

where $k_0=\omega_T\epsilon_b^{1/2}/c$ and $v_{G_0}=v_G(\omega_T)$ have been introduced for normalization purposes. Since the density of states for the lower polariton branch is a monotonically increasing function of ω, the damping constant $\gamma(\omega)$ and the Brillouin linewidth will therefore increase with increasing frequency. Figure 2(b) shows the best fit to model II with the constants

$$\tilde{\gamma}_0=0.117\ \mathrm{cm}^{-1},\ \ \tilde{\gamma}_1=0.345\ \mathrm{cm}^{-1}\ . \tag{8}$$

The $\gamma(\omega)$ of Eq. (7) fits the observed linewidth better than γ_0 alone, but is still not satisfactory.

It should be noted that if the intrabranch decay of polaritons came primarily from acoustic-phonon scattering, which conserves energy and momentum, the second term of Eq. (7) would be[12]

$$\begin{aligned}\gamma_1(\omega)&\propto\int|\Gamma_0(\vec{q})|^2\delta(\hbar\omega_I-\hbar\omega_S-\hbar c|\vec{q}|)d\vec{q}\\&\propto k'(\omega)^2\end{aligned} \tag{9}$$

instead of $[k'(\omega)]^2/|v_G(\omega)|$. However, since $[k'(\omega)]^2$ increases more slowly than $[k'(\omega)]^2/|v_G(\omega)|$, the linewidth calculated using Eq. (9) was found to give a worse fit to the data than that shown in Fig. 2(b).

Next, we consider the third term [term (iii)] in $\gamma(\omega)$. It was first shown by Hopfield and Thomas that a perturbation can exist for electron or hole (as well as exciton) states with nonzero wave vector which is proportional to $k_\perp$.[10] The existence of such an interaction was verified experimentally in the reflectivity spectrum of CdS in the region of the B exciton. From symmetry considerations, however, the k-linear interaction can mix $\Gamma_6(A)$ spin-triplet and $\Gamma_{5\mathrm{T}}(A)$ spin-singlet exciton states as well.[17] In the presence of this interaction, three modes must be included in the calculation: $\Gamma_{5\mathrm{T}}(A)$ and $\Gamma_6(A)$ excitons, and photons. Instead of the two-branch dispersion curves given by Eq. (4), one then has three-branch dispersion curves which are the solutions to the following equation:[18]

$$\begin{array}{c}\begin{array}{ccc}|\Gamma_{5T}(A)\rangle & |\Gamma_6(A)\rangle & |\mathrm{photon}\rangle\end{array}\\ \left|\begin{array}{ccc}\omega_T+B_5k^2-i\gamma/2-\omega & -iek & (2\pi\alpha_0\omega_T)^{1/2}\\ iek & \omega_6+B_6k^2-i\gamma_6/2-\omega & 0\\ (2\pi\alpha_0\omega_T)^{1/2} & 0 & -\epsilon_b+k^2c^2/\omega^2\end{array}\right|=0\ ,\end{array} \tag{10}$$

where $B_5=\hbar/2m^*$, $B_6=\hbar/2m_6^*$, $\omega_6=\omega_T-\Delta_{56}$, m_6^* and γ_6 are the effective mass and damping constant of the $\Gamma_6(A)$ state, Δ_{56} is the frequency difference between the singlet $\Gamma_{5\mathrm{T}}(A)$ and triplet $\Gamma_6(A)$ exciton states at $\vec{k}=0$, and e is the coefficient of the k-linear interaction. In the following calculation we take[19] $\tilde{\Delta}_{56}=1.6\ \mathrm{cm}^{-1}$ and assume that $m_6^*=m^*(\Gamma_5)=0.83m_0$. Equation (10) can be solved as a function of real frequency ω by reducing it to an eigenvalue problem with respect to the complex wave vector k.[18] Figure 3 shows the dispersion curves for the three branches Γ_α, Γ_β, and Γ_γ, the last of which is almost the same as the usual upper polariton branch (1) in the two-branch theory of Eq. (4). These curves $k'(\omega)$ are again insensitive to the damping constants $\tilde{\gamma}$ and $\tilde{\gamma}_6$, which have both been taken as 0.5 cm^{-1} in the calculation leading to Fig. 3.

Since the $\Gamma_6(A)$ frequency $\tilde{\omega}_6$ at $\vec{k}=0$ is 1.6 cm^{-1} *below* the $\Gamma_{5\mathrm{T}}(A)$ exciton, the lower two branches would cross at $\omega_{\mathrm{cr}}\approx 20\,594\ \mathrm{cm}^{-1}$, but the k-linear interaction converts this to an anticrossing. Most polaritons are created on the Γ_β branch for $\omega>\omega_{\mathrm{cr}}$ and on the Γ_α branch for $\omega<\omega_{\mathrm{cr}}$ because Γ_6 excitons do not couple to photons. To first approximation we neglect the upper polariton branch Γ_γ and consider the mixing of Γ_6 excitons with lower-branch polaritons (Γ_{5l}). Since the exciton-strength function[11] $A_{22}\approx 1$ for $\omega\approx\omega_{\mathrm{cr}}$, the k-linear interaction between these two branches is still iek. A simple perturbation calculation for these two states with the same $\vec{k}$ gives

$$|\Gamma_\alpha(A)\rangle=C_{\alpha 5}|\Gamma_{5l}(A)\rangle+C_{\alpha 6}|\Gamma_6(A)\rangle\ , \tag{11a}$$

with

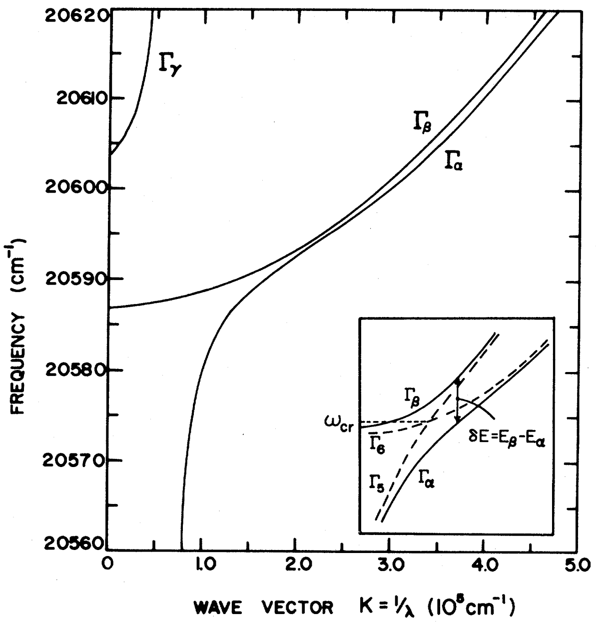

FIG. 3. Calculated dispersion curves of $\Gamma_5(A)$ exciton-polaritons and $\Gamma_6(A)$ excitons including the k-linear interaction term between the $\Gamma_5(A)$ and $\Gamma_6(A)$ excitons. Inset: Schematic representation of the dispersion curves near the crossing frequency ω_{cr}. The dashed lines show the lower-branch $\Gamma_{5l}(A)$ polariton and $\Gamma_6(A)$ exciton without the k-linear interaction.

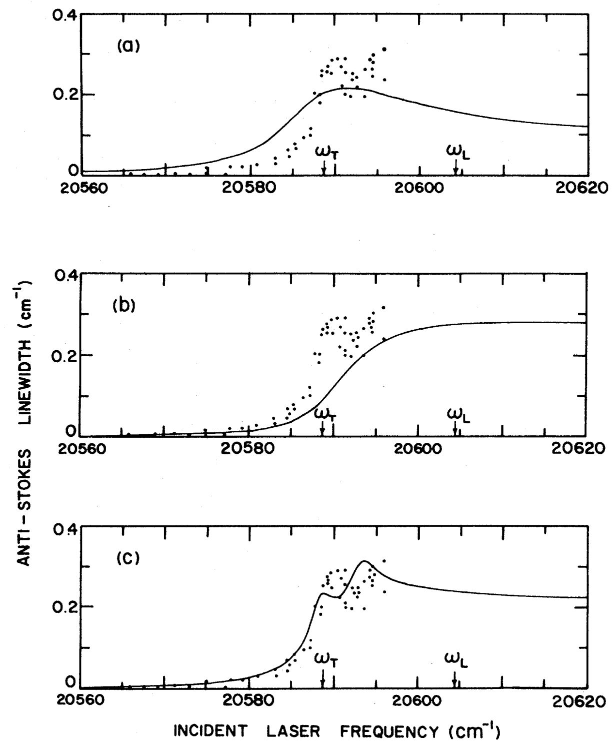

FIG. 4. Anti-Stokes LA 2-2′ Brillouin linewidth vs incident laser frequency. The dots are the experimental data. The lines are theoretical predictions using the parameters found from the Stokes LA 2-2′ fits given in the caption of Fig. 2.

$$|C_{\alpha 6}|^2=\frac{e^2|\vec{k}|^2}{(E_\alpha-E_6)^2+e^2|\vec{k}|^2}, \tag{11b}$$

where Γ_{5l} is the lower-branch polariton of the Γ_5 transverse exciton, and $E_\alpha - E_6$ is the energy difference between the perturbed Γ_α state and the unperturbed Γ_6 state. The fraction of Γ_6 in the mixed Γ_β state is given by Eq. (11) with α replaced by β. This Γ_6 part of the polariton can decay to other states on the Γ_6-exciton branch via successive interactions with acoustic phonons or defects. Thus, the wave-vector-induced interaction can open an extra decay channel for polaritons with $\omega \approx \omega_{cr}$. In view of the simplified model adopted here, for $\omega < \omega_{cr}$ we approximate the energy difference $|E_\alpha - E_6|$ by $\delta E = E_\beta - E_\alpha$ calculated at $k'(\omega)$ of the unperturbed lower-branch polariton Γ_{5l} (see Fig. 3) and take $\gamma \propto |C_{\alpha 6}|^2$. For $\omega > \omega_{cr}$, we approximate the energy difference $|E_\beta - E_6|$ by δE and take $\gamma \propto |C_{\beta 6}|^2$. We then use the following form for the total damping constant $\gamma(\omega)$ (model III):

$$\gamma(\omega)=\gamma_0+\gamma_1[k'(\omega)/k_0]^2[v_{G_0}/v_G(\omega)] +\gamma_2[e\,|k(\omega)|\,]^2/\{\,|\delta E(\omega)|^2+[e\,|k(\omega)|\,]^2\}. \tag{12}$$

The three terms on the right-hand side of Eq. (12) correspond to the three decay mechanisms (i), (ii), and (iii) discussed previously in this section. The solid line in Fig. 2(c) is the best fit to Eq. (12), with

$$\tilde{\gamma}_0=0.241\ \text{cm}^{-1},\ \tilde{\gamma}_1=0.091\ \text{cm}^{-1}, \quad \tilde{\gamma}_2=2.691\ \text{cm}^{-1},\ e=2.85\times 10^4\ \text{cm/sec}. \tag{13}$$

It is seen that the frequency dependence of the Brillouin linewidth including the rapid increase near ω_{cr} is well fitted by the model-III $\gamma(\omega)$ of Eq. (12). The two peaks which appear in the theoretical linewidth represent the increased damping when either the incident- or scattered-polariton frequency coincides with the frequency of strongest mixing, ω_{cr}. Although two peaks are not clearly seen in the data, a slight decrease in the linewidth was observed at about 20 598 cm^{-1} for the Stokes component (Fig. 2) and at about 20 593 cm^{-1} for the anti-Stokes component (Fig. 4). For higher frequencies, a rapid decrease in the RBS intensity as well as increasingly serious local heating (even with only 8 mW of laser power) made accurate measurement of the linewidth very difficult.

B. Linewidth of anti-Stokes LA 2-2′ Brillouin component

The linewidths of the anti-Stokes LA 2-2′ Brillouin components were also measured and are shown by the dots in Fig. 4. The sharp increase in linewidth occurs approximately 5 cm^{-1} lower in frequency than for the Stokes component since, for anti-Stokes scattering, the scattered polariton has higher frequency than for Stokes scattering.

Using the parameters determined from the Stokes spectra [given in Eqs. (6), (8), and (13)], the anti-Stokes linewidth was calculated for the three models for $\gamma(\omega)$ discussed above. The calculated linewidths are shown by the solid curves in Figs. 4(a)—4(c). Again, the frequency-indepenent damping constant γ_0 of model I [Eq. (6)] or the $\gamma(\omega)$ of model II [Eq. (8)] give poor fits to the data, while model III [Eq. (13)] agrees reasonably well with the measured linewidth.

C. RBS intensity

The frequency-dependent damping constant $\gamma(\omega)$ and the additional boundary condition (ABC) critically affect the RBS intensity given by Eq. (5). Here, we present a preliminary analysis using a generalized ABC together with $\gamma(\omega)$ determined from the linewidth analysis discussed above.

Three ABC's have been used most frequently to compare theory and experiments. These are the ABC given by Pekar[20] [$\sum_{i=1}^{2}(P_i)_{x=0}=0$, denoted ABC1 in Refs. 3 and 11], ABC2 given by Ting *et al.*[21,22] [$\sum_{i=1}^{2}(dP_i/dx)_{x=0}=0$], and the dielectric approximation (ABC3) in which the bulk nonlocal susceptibility for an exciton is assumed to be valid in the entire crystal up to the boundary.[23]

The RBS intensity of Stokes LA 2-2$'$ Brillouin scattering was measured by integrating the area under each Brillouin component in the raw spectrum. The intensity data were compared with the theory[11] with ABC's 1, 2, and 3, with the $\gamma(\omega)$ given in Eqs. (12) and (13). As seen in Fig. 5(a), none of these commonly used ABC's agrees very well with the data.

It has been noted[9] that these three ABC's are special cases of a generalized form of ABC including a parameter a,

$$\sum_{i=1}^{2}\left[P_i(x)+a\left[\frac{dP_i}{dx}\right]\right]_{x=0}=0\ . \tag{14}$$

The equivalent condition on the exciton wave function $\phi_k(x)$ is[22]

$$\phi_k(x)=(e^{-ik_ex}+se^{ik_ex})\Theta(x)\ , \tag{15}$$

where s is the exciton-reflection parameter and $\Theta(x)$ is the usual unit step function. The reflection parameter s is related to the parameter a in Eq. (14) by

$$s=(iak_e-1)/(iak_e+1)\ , \tag{16}$$

where k_e is the bare exciton wave vector and $s=-1$, $+1$, and 0 corresponds to ABC 1, 2, and 3, respectively.

A further modification to the generalized ABC formalism was recently proposed by Nakayama.[13] In his theory, an evanescent wave $\exp(-x/b)$ was introduced to make the total polarization vanish at the boundary. The parameter b may be considered as an effective dead-layer thickness in which the orbital wave function of the exciton differs significantly from the $1s$ function in the bulk crystal far from the boundary.

Considering s and b as adjustable parameters in the ABC, the observed RBS intensity was fitted using $\gamma(\omega)$ determined from the linewidth analysis with models I, II, and III. Again, the $\gamma(\omega)$ of model III, which includes all three decay mechanisms, gave the best fit, as shown in Fig. 5(b). The ABC parameters determined by the fit were

$$s=1.0e^{1.84\pi i},\quad b=0.23\ \text{Å}\ . \tag{17}$$

This result indicates that the dead-layer effect is very

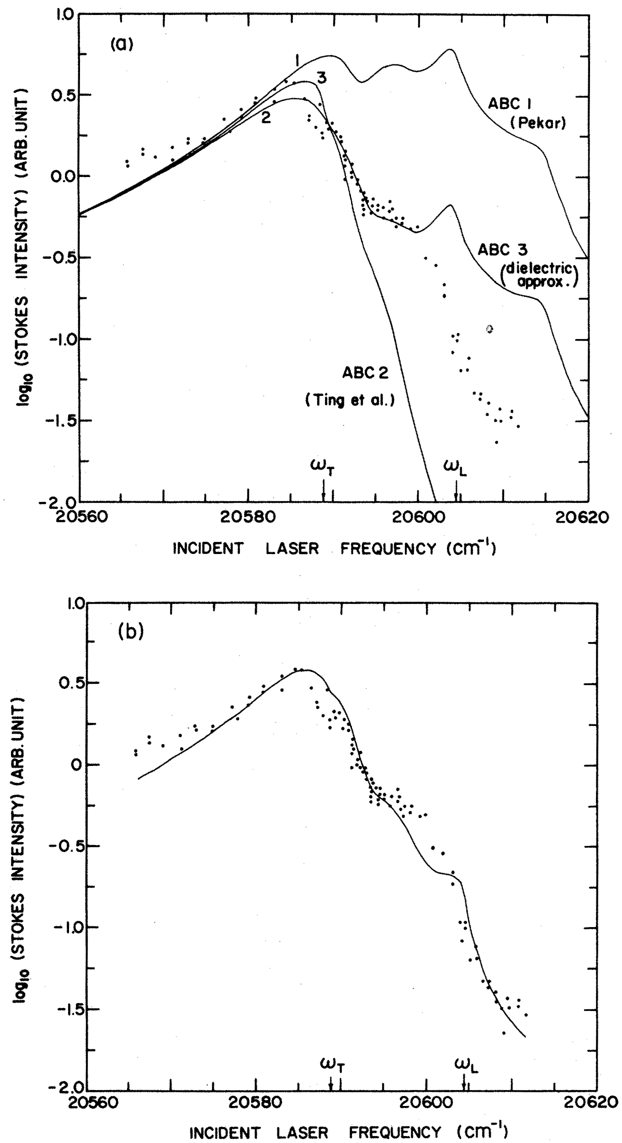

FIG. 5. (a) Logarithm of the integrated intensity of Stokes LA 2-2$'$ Brillouin scattering peaks vs incident laser frequency. The dots are the experimental data. The lines are the calculated result using $\gamma(\omega)$ given by Eq. (12) (model III) with ABC 1, 2, and 3, respectively. The dead-layer thickness is taken as zero. (b) Logarithm of the integrated intensity of Stokes LA 2-2$'$ Brillouin scattering peaks vs incident laser frequency. The dots are the experimental data. The line is the best-fit result to Nakayama's generalized ABC with $S=1.0\exp(i\,1.84\pi)$ and $b=0.23$ Å, with $\gamma(\omega)$ given by Eqs. (12) and (13).

small and that the appropriate ABC is close to ABC2 of Ting *et al.*, but falls between ABC2 and ABC1.

IV. DISCUSSION

A. Lifetime of polaritons

The damping constants $\gamma(\omega)$ found from fitting the RBS-linewidth data to models I, II, and III are plotted in Fig. 6. Let us compare these results to polariton lifetimes obtained from luminescence experiments. In their luminescence experiment, Wiesner and Heim excited polaritons with a picosecond laser pulse at 457.9 nm (21 839 cm^{-1}), which is well above ω_T, and measured the exponential decay of the luminescence at various energies.[8] Their result, reproduced in Fig. 7(b), shows that in the vicinity of ω_T, τ_{lum} increases with decreasing frequency from almost 0 ns (less than the experimental resolution of 0.3 ns) up to about 3 ns for observation frequencies below ω_T. This inrease of τ_{lum} has been attributed to the onset of the bottleneck effect in polariton decay.

Sumi made a numerical evaluation of the polariton lifetime to explain the intensity ratio of zero-phonon and one-LO-phonon luminescence.[24] His result implies that $\tau \approx 10^{-9}$ to 10^{-10} s with a maximum of about 1 ns at frequencies several cm^{-1} below ω_T. In contrast to the long lifetimes measured by luminescence, $\tau(\omega)=2/\gamma(\omega)$ determined from the present RBS experiments is about 2 orders of magnitude shorter.[25] The experimental linewidth of RBS in GaAs has been reported[4] to increase from about 0.02 to 0.3 cm^{-1}, which is similar to our results for CdS.

The difference between τ_{lum} and τ_{RBS} could be attributed in part to the fact that τ_{RBS} is the lifetime of a polariton created directly at a specific ω and k, while τ_{lum} is a *net* lifetime determined by the balance between polaritons entering and leaving a particular energy range. Thus, τ_{lum} includes the sum of the contributions of all decay paths which produce polaritons in states with a given ω. Another important difference between RBS and luminescence lifetimes is that a polariton that undergoes elastic scattering which changes the direction of k without changing ω can still contribute to luminescence, but *not* to RBS. In RBS, the initial and final states are specified and any polariton scattering process, including elastic scattering from defects, internal stress etc., reduces the RBS lifetime.

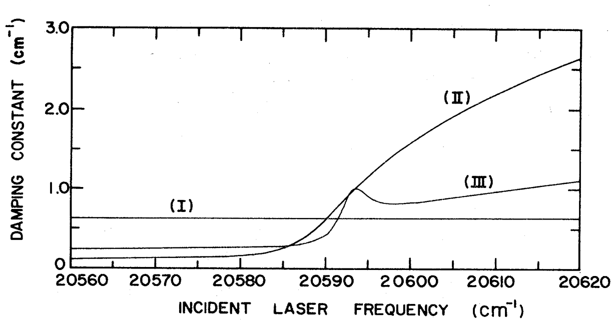

FIG. 6. Frequency dependence of the damping constant $\gamma(\omega)$ found from the Brillouin linewidth data with models I [Eq. (6)], II [Eq. (7)], and III [Eq. (12)].

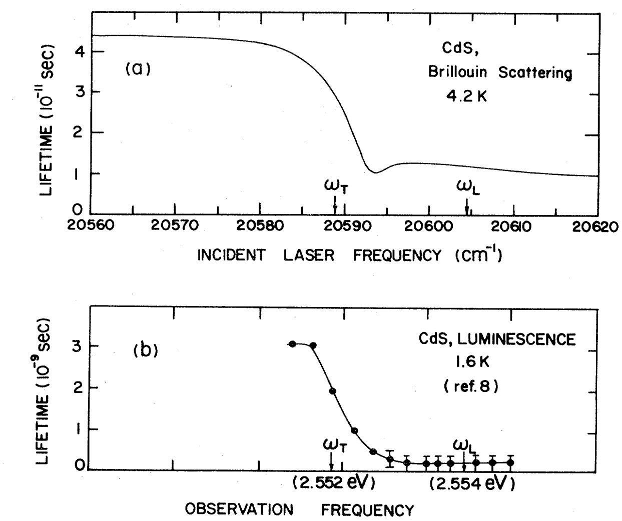

FIG. 7. (a) Lifetime of polaritons corresponding to the $\gamma(\omega)$ obtained from the best fit of the RBS-linewidth data to model III. (b) Polariton lifetime measured by Wiesner and Heim with time-resolved luminescence spectroscopy (from Ref. 8).

Recently, Askary and Yu measured CdS luminescence by a method similar to that of Wiesner and Heim and found that there are two lifetimes, τ_{fast} and τ_{slow}.[27] However, their τ_{fast} is still several tenths of a nanosecond and is much longer than τ_{RBS}. When the elastic scattering rate [the second term in Eq. (12)] is dominant, i.e., when relaxation between states of the same energy occurs much faster than other relaxation processes, τ_{RBS} can be much shorter than τ_{lum}. However, our result [Eq. (13)] for $\gamma(\omega)$ indicates that processes other than elastic scattering also contribute significantly to τ_{RBS}. Therefore, the origin of the large difference between τ_{RBS} and τ_{lum} is not yet entirely clear.

In spite of the difference in magnitude between the two lifetimes, τ_{RBS} also shows an increase of lifetime with decreasing ω near ω_T corresponding to the onset of the bottleneck effect for lower-branch polaritons due to the rapid change in the density of states. It should be noted that in luminescence experiments the lifetime is too short to be measured for frequencies $\omega > \omega_T$, while RBS line broadening is measurable in the region between ω_T and ω_L, which is important for the ABC problem.

Recently, Masumoto *et al.*[28] measured the relaxation of exciton-polaritons in CuCl by time-resolved four-wave—mixing spectroscopy. They identify γ, defined similarly to our Eq. (4), as a dephasing damping constant (or transverse relaxation rate in a two-level system.) Since elastic scattering of polaritons causes dephasing of a light pulse propagating coherently in a given direction, one may expect that the damping observed in their experiment would show behavior similar to that obtained from RBS experiments. They observed an increase of $\tilde{\gamma}$ from 0.1 cm^{-1} well below $\tilde{\omega}_T$ to about 1.0 cm^{-1} in the resonance region, which corresponds to the same order-of-magnitude lifetime as $\tau_{\rm RBS}$. Because of the large scatter in the data, however, it is very difficult to determine the frequency dependence of $\gamma(\omega)$ from four-wave–mixing experiments.

B. Linewidth expression in RBS

So far we have assumed that the RBS linewidth is given by Eq. (3) with k determined by Eq. (4). Dervisch and Loudon have shown that if phonon reflection at the crystal surface is taken into account, the line shape of RBS cannot be a simple Lorentzian and should be a skewed Lorentzian instead.[29] According to their result and its extension by Tilley to the case of RBS via exciton polaritons,[30] the linewidth is still given by Eq. (3) if the interference between scattering involving different polariton branches can be ignored. Since the LA 2-2′ peak is well isolated from other components and no line-shape distortion was observed, we believe that the linewidth formula Eq. (3) can still be used for this case.

In Eq. (1) we have also neglected the frequency dependence of the transmissivity $T(\omega)$ when we calculate the linewidth. Actually, $T(\omega)$ changes considerably between ω_T and ω_L depending on the ABC. However, numerical evaluation[11] for different ABC's shows that a change of 50% in $T(\omega)$ occurs over a frequency range of at least 5 $\rm cm^{-1}$, which is much larger than the typical Brillouin linewidth (less than 0.5 $\rm cm^{-1}$). Therefore the frequency dependence of the transmissivity and the ABC which determiness it have little effect on the RBS linewidth.

C. Wave-vector-induced mixing of exciton states

For $\vec{k}=(k,0,0)$, wave-vector-induced mixing involving A and B excitons in CdS can occur in the following cases:[17] (i) between A and B excitons, $\Gamma_{5L}(A)$ and $\Gamma_1(B)$ (where L denotes longitudinal) as suggested by Hopfield and Thomas,[31] or $\Gamma_6(A)$ and $\Gamma_5(B)$; (ii) among different B-exciton states, $\Gamma_{5T}(B)$ and $\Gamma_2(B)$, or $\Gamma_{5L}(B)$ and $\Gamma_1(B)$, which was treated by Mahan and Hopfield;[32] (iii) among the A-exciton states, $\Gamma_{5T}(A)$ and $\Gamma_6(A)$, or $\Gamma_{5L}(A)$ and $\Gamma_6(A)$. The effects considered in Sec. III correspond to case (iii). Although this case was suggested as a possible explanation for magnetoluminescence observations in the configuration $\vec{E}\perp\hat{c}$ and $\vec{H}\|\hat{c}$,[33] no explicit evidence for k-linear interactions among the A-exciton states has been reported to date.

It should be noted that in the third term of Eq. (12), which gives the contribution to $\gamma(\omega)$ of the k-linear interaction, $\delta E(\omega)$ and $k(\omega)$ are not adjustable but were calculated using only predetermined constants. In particular, $\tilde{\Delta}_{56}=1.6\ \rm cm^{-1}$ [frequency difference between $\Gamma_{5T}(A)$ and $\Gamma_6(A)$ at $\vec{k}=\vec{0}$] (Ref. 19) and $m^*(\Gamma_6)=0.83m_0$ [equal to $m^*(\Gamma_5)$] have been fixed. Those parameters determine the level-crossing frequency $\omega_{\rm cr}$ (Fig. 3) where the wave-vector-induced mixing is greatest. To check the value of $\omega_{\rm cr}$ separately, we applied a weak magnetic field (1.3 T) along the y direction ($y\perp c$ and $\vec{k}$) which also mixes the $\Gamma_{5T}(A)$ and $\Gamma_6(A)$ states most strongly at $\omega_{\rm cr}$ and can Zeeman-split the RBS spectra as well. Clear broadening of the Brillouin lines (rather than the splitting which would be observed with stronger magnetic fields) was observed only when $\tilde{\omega}_{\rm inc}$ or $\tilde{\omega}_{\rm sc}$ was close to 20 594 $\rm cm^{-1}$.

Our result for the k-linear coefficient of A-excitons in CdS agrees reasonably well with the value determined from the literature. Recent spin-flip Raman scattering experiments by Romestain *et al.*[34] gave the k-linear coefficient of the Γ_7 conduction band as $C_e=1.6\times10^{-11}$ eV cm, while the Γ_9 symmetry of the valence band requires that its k-linear coefficient vanishes, $C_h=0$. The k-linear coefficient of the A-exciton is given by[35]

$$\phi_A=(C_h m_{h\perp}^A - C_e m_{e\perp})/(m_{h\perp}^A + m_{e\perp})\ .$$

Using $m_{e\perp}=0.208m_0$, and $m_{h\perp}^A=0.68m_0$,[31] we obtain

$$|\phi_A|=3.8\times10^{-11}\ \text{eV cm}\ ,$$

which agrees within a factor of 2 with our experimental result,

$$|\phi_A|=\hbar e=1.9\times10^{-11}\ \text{eV cm}\ .$$

It should be noted that the k-linear effect for the A exciton is $\sim$20 times weaker than for the B exciton[35] and corresponds to an effective magnetic field of only 3.6 kG. This is too small to cause any observable splitting of exciton levels or reflectivity anomalies. However, it is sufficiently big to cause significant broadening of the Brillouin components in the vicinity of $\omega_{\rm cr}$.

In conclusion, we have shown that the RBS-linewidth measurement implies that the phenomenological damping constant $\gamma(\omega)$ depends on frequency in a rather complicated way. In order to explain the sharp increase of the linewidth above the exciton resonance frequency ω_T, the decay of $\Gamma_{5T}(A)$ polaritons to $\Gamma_6(A)$-exciton states via the wave-vector-induced interaction has been proposed. Detailed linewidth measurements with stronger magnetic fields would be helpful to further clarify this mechanism.

The frequency-dependent damping constant $\gamma(\omega)$ is also crucial in the analysis of RBS intensity, from which it may be possible to resolve the still controversial ABC problem of spatially dispersive media. Our preliminary fitting presented in this paper indicates that none of the three commonly used ABC's agree with experiment and suggests the need for the generalized ABC of Nakayama.[13] Further experiments in stronger magnetic fields are in progress and will be reported in a subsequent publication.

ACKNOWLEDGMENTS

We are grateful to M. Matsushita and J. Wicksted for valuable discussions and for their participation in the early stages of this work. We thank J. L. Birman for stimulating discussions and advice, and P. Y. Yu for helpful suggestions and for providing unpublished reports of his luminescence studies prior to publication. We also thank M. Nakayama for an interesting discussion and for providing a copy of his unpublished manuscript on the generalized ABC prior to publication. This research was supported by the National Science Foundation under Grant No. DMR-80-20835.

*Permanent address: Department of Engineering Physics and Institute of Laser Sciences, The University of Electro-Communications, 1-5-1 Chofugaoka, Chofu-shi, Tokyo 182, Japan.

[1]W. Brenig, R. Zeyher, and J. L. Birman, Phys. Rev. B **6**, 4617 (1972).

[2]See the review articles by P. Y. Yu, in *Light Scattering in Solids,* edited by J. L. Birman, H. Z. Cummins, and K. K. Rebane (Plenum, New York, 1979), p. 143; E. S. Koteles, in *Excitons,* edited by E. I. Rashba and M. D. Sturge (North-Holland, Amsterdam, 1982), p. 83; R. B. Ulbrich and C. Weisbuch, in *Festkörperprobleme (Advances in Solid State Physics),* edited by J. Treusch (Vieweg, Braunschweig, 1978), Vol. XVIII, p. 217.

[3]J. Wicksted, M. Matsushita, H. Z. Cummins, T. Shigenari, and X. Z. Lu, Phys. Rev. B **29**, 3350 (1984).

[4]C. Weisbuch and R. G. Ulbrich, in *Proceedings of the International Conference on Lattice Dynamics, Paris, 1977,* edited by M. Balkanski (Flammarion, Paris, 1978), p. 167; C. Hermann and P. Y. Yu, Solid State Commun. **28**, 313 (1978).

[5]J. Wicksted, M. Matsushita, and H. Z. Cummins, Solid State Commun. **38**, 777 (1981).

[6]Y. Toyozawa, Prog. Theor. Phys. Suppl. **12**, 111 (1959).

[7]C. Benoit a la Guillaume, A. Bonnot, and J. M. Deberer, Phys. Rev. Lett. **24**, 1235 (1970).

[8]P. Wiesner and U. Heim, Phys. Rev. B **11**, 3071 (1975).

[9]See the review article by J. L. Birman, in *Excitons,* Ref. 2.

[10]J. J. Hopfield and D. G. Thomas, Phys. Rev. **132**, 563 (1963).

[11]M. Matsushita, J. Wicksted, and H. Z. Cummins, Phys. Rev. B **29**, 3362 (1984).

[12]P. Y. Yu and Y. R. Shen, Phys. Rev. B **12**, 1377 (1975).

[13]Y. Segawa, Y. Aoyagi, S. Komuro, S. Namba, S. Inoue, and M. Nakayama (unpublished); M. Nakayama *et al.* (unpublished).

[14]E. J. Flynn and S. Geschwind, Bull. Am. Phys. Soc. **26**, 488 (1981).

[15]J. R. Sandercock, Phys. Rev. Lett. **29**, 1735 (1972).

[16]It can be easily seen from Eq. (4) that, in the absence of damping, the wave vector of the lower-branch polariton has no imaginary part at any frequency.

[17]K. Cho, Phys. Rev. B **14**, 4463 (1976).

[18]K. Cho, Solid State Commun. **27**, 205 (1978).

[19]I. Broser and M. Rosenzweig, Phys. Rev. B **22**, 2000 (1980).

[20]S. I. Pekar, Zh. Eksp. Teor. Fiz. **33**, 1022 (1957) [Sov. Phys.—JETP **6**, 785 (1958)].

[21]C. S. Ting, M. Frankel, and J. L. Birman, Solid State Commun. **17**, 1285 (1975).

[22]R. Zeyher, J. L. Birman, and W. Brenig, Phys. Rev. B **6**, 4613 (1972).

[23]J. L. Birman and J. J. Sein, Phys. Rev. B **6**, 2482 (1971); A. A. Maradudin and D. L. Mills, *ibid.* **7**, 2787 (1973); G. S. Agarwal, D. N. Pattanayak, and E. Wolf, Phys. Rev. Lett. **27**, 1022 (1971).

[24]H. Sumi, Solid State Commun. **17**, 701 (1975); J. Phys. Soc. Jpn. **41**, 526 (1976).

[25]Generally speaking, the lifetime depends on the quality of the sample. However, Yu (Ref. 26) has measured the luminescence from a sample with the same origin as ours and found lifetime of a few nanoseconds, similar to the values of Wiesner and Heim (Ref. 8).

[26]P. Y. Yu (private communication).

[27]F. Askary and P. Y. Yu, Phys. Rev. B **28**, 6165 (1983).

[28]Y. Masumoto, S. Shionoya, and T. Takagahara, Phys. Rev. Lett. **51**, 923 (1983).

[29]A. Dervisch and R. Loudon, J. Phys. C **9**. L669 (1976).

[30]D. R. Tilley, J. Phys. C **13**, 781 (1980).

[31]J. J. Hopfield and D. G. Thomas, Phys. Rev. **122**, 35 (1961).

[32]G. D. Mahan and J. J. Hopfield, Phys. Rev. **135**, A428 (1964).

[33]H. Venghaus, S. Suga, and K. Cho, Phys. Rev. B **16**, 4419 (1977).

[34]R. Romestain, S. Geschwind, and G. E. Devlin, Phys. Rev. Lett. **39**, 1583 (1977).

[35]E. S. Koteles and G. Winterling, Phys. Rev. Lett. **44**, 948 (1980).